

ANALYSIS OF ERRORS OF MULTIBLOCK COMPUTATIONAL TECHNOLOGIES BY THE EXAMPLE OF CALCULATING A CIRCULATION FLOW IN A SQUARE CAVITY WITH A MOVING COVER AT $Re = 10^3$

S. A. Isaev,^a A. G. Sudakov,^b P. A. Baranov,^b
Yu. V. Zhukova,^c and A. E. Usachov^d

UDC 532.517:2

The errors of multiblock computational technologies realized in different versions of the VP2/3 package and involving the use of structured computational meshes of the H and O types with superposition were methodically investigated by the example of solving the problem on a circulation flow of an incompressible viscous fluid in a square cavity with a moving cover at a moderate Reynolds number of $\sim 10^3$. A comparison of the numerical estimations of the integral and extremum local characteristics of the indicated flow, made with the use of composite and multiblock meshes with varying densities and near-wall steps, has shown that it is reasonable to use multiblock computational technologies with linear interpolation in the calculations with conversion of parameters from mesh to mesh.

Keywords: *circulation flow, cavity, calculation, procedure of pressure correction, Rhie–Chow approach, multiblock computational technologies, VP2/3 package.*

Introduction. Package technologies used for solving problems of aerohydraulics and heat exchange represent a powerful instrument of basic and applied research that successfully supplements analogous experimental means. Among the widely used program packages, the universal commercial Fluent and CFX packages with a closed (for users) "core" and open-type packages, e.g., the OPEN FOAM package, whose codes are accessible on the Internet, stand out. In these packages, computational subregions are divided as a rule by multiblock meshes with common boundaries, which sometimes leads to an increase in the bevel angles of the generated cells and to significant errors in the numerical simulation.

An alternative approach based on multiblock computational technologies (MCT) involves solution of initial equations with the use of composite meshes, in which simple-topology meshes of the H and O types are superimposed and intersected. Multiblock computational technologies are realized using the specialized velocity-pressure (VP) package in the two-dimensional and three-dimensional versions [1, 2]. The MCT conception was initially associated with the construction of near-orthogonal algebraic meshes superimposed on each other with intersection for description of flows in multiply connected computational regions [3]. The development of multiblock computational technologies has made it possible to calculate the flow about a body with built-in vortex cells, investigate the effect of decreasing the drag of a circular cylinder and a thick profile, and increase the lifting force acting on a profile by control of the circulation flow about it and partial or complete prevention of its separation on the backside of the body [4]. It is significant that, in this case, different-scale structured meshes with steps changing spasmodically from subregion to subregion are used, which makes it possible to easily pass from the consideration of complex-geometry streamlined objects to the less obvious reproduction of the different-scale elements of a flow on the specially introduced meshes of corresponding scale. In the problems on the vortex intensification of the heat exchange in holes, of importance is the representation of both the high-gradient flows in the vicinity of the rounded edges of the holes and the spiral-like vortex structures in the near wake downstream of them, for identification of which special meshes are introduced [5–7]. The discussion presented in [8] once again called attention to the analysis of the errors of multiblock computational technologies that arise as a result of the conversion of parameters from mesh to mesh, especially in the case where meshes of different types with different densities are used. Therefore, it makes sense to test multiblock

^aSt. Petersburg State University of Civil Aviation, 38 Pilotov Str., St. Petersburg, 196210, Russia; ^bAccumulator Company "Riegel," 38 Prof. Popov Str., St. Petersburg, 197376, Russia; ^cA. V. Luikov Heat and Mass Transfer Institute, National Academy of Sciences of Belarus, 15 P. Brovka Str., Minsk, 220072, Belarus; ^dBranch of the Central Aerohydrodynamic Institute "Moscow Complex," 17 Radio Str., Moscow, 105005, Russia; email: isaev3612@yandex.ru. Translated from *Inzhenerno-Fizicheskii Zhurnal*, Vol. 86, No. 5, pp. 1064–1079, September–October, 2013. Original article submitted April 30, 2013.

computational technologies and different modifications of the VP2/3 package by the example of solving the classical problem on the circulation flow of a viscous incompressible fluid in a square cavity with a moving cover, for which a considerable amount of recent calculation data has been accumulated [9, 10]. Since, in the previous investigations, emphasis was placed on the variations of the density and the near-wall step of a multiblock mesh as well as on increasing the Reynolds-number range to $6 \cdot 10^4$, in the present work we introduced additional meshes of the H and O type and analyzed the influence of the parameters of the external and internal meshes on the integral and local characteristics of the flow in a square cavity with a moving cover at $Re = 10^3$.

Investigation Object. The problem on the circulation flow of an incompressible viscous fluid in a square cavity, initiated by the movement of its upper solid wall with a constant velocity, is considered. For a long time, this problem was used as a basis for development of methods for solving Navier–Stokes equations. In the late 1960s — early 1970s, the calculation possibilities of computers not only provided no way of using fine meshes (the number of mesh nodes was limited by several hundreds) but also forced one to decrease the number of dependent variables by writing the initial equations in transformed variables, e.g., in vorticity–stream function ones [11–13]. Despite the limitedness of the computational resources, one of the most important problems in solving numerically the Navier–Stokes equations, associated with the presence of the small parameter at the higher derivative, was solved. The requirement for the stability of the computational process dictated the use of upwind schemes of the first-order accuracy, in particular the Spaulding scheme [12, 14]. In this case, the errors in the approximation of the convective numbers of the vortex-transfer equation give birth to the numerical diffusion that is proportional to the local velocity of the flow, the step of the mesh being used, and the bevel-angle of the flow relative to the mesh lines [15]. At large Reynolds numbers, this diffusion exceeds the physical diffusion. Therefore [9], the scheme errors cannot be eliminated by increasing the density of the mesh, and, at a moderate Reynolds number $Re = 10^3$, the asymptotic value of the rate of flow of a viscous incompressible fluid involved in the circulation motion initiated by the moving cover is markedly smaller (smaller than 0.1 in fractions of the product of the characteristic velocity of the flow by the length of the cavity face) than in the case where more exact algorithms are used ($|\psi_m| = 0.1191$).

It has been possible to overcome the distorting influence of the numerical diffusion on the solution of the Navier–Stokes equations with the use of high-order schemes, e.g., Arakawa schemes of the second and fourth orders of approximation [16, 17], the Agarwal upwind scheme of the third order of approximation [18], Leonard’s upwind scheme with quadratic interpolation [19], and schemes of the fourth order of approximation described in [20]. The progress in computer engineering and then the computer boom made it possible not only to refine computational meshes, but also to solve equations written in natural variables. This approach is more easily generalized to the spatial case, and the boundary conditions set at the wall are simpler. During the several last decades, a number of monographs on the methodology of solving the equations of hydromechanics in natural variables have been published [21–23]. These monographs form the information basis for the development of applied-program packages (package technologies) realized with the use of the finite-volume method and the pressure-correction algorithms based on the concept of splitting by physical processes. In one of the first detailed methodological investigations of the problem being considered [24], the solutions of the Navier–Stokes equations for different dependent variables and digitization schemes with varying mesh parameters were compared. Particular emphasis was placed on the use of staggered and centered templates for disposition of dependent variables. It should be noted that the disposition of all the variables at the center of a cell of a structured or a nonstructured mesh is generally accepted now.

The problem on the flow of an incompressible viscous fluid in a square cavity with a moving cover has always received the attention of researchers, because, in this case, a simple computational region and an orthogonal computational mesh can be used, despite the cone features of the problem associated with the drop in the velocity of the flow at the upper cone points of the cavity and the absence, by this reason, of a physical analog of such a flow. However, this classical problem attracted the interest of researchers even before the numerical-simulation age, first of all, due to the Batchelor hypothesis on the formation of a nonviscous vortex surrounded by a thin boundary layer in such a cavity at ultimately large Reynolds numbers $Re \rightarrow \infty$. This hypothesis was confirmed to some extent for a circular cavity by Squire [25]. An effort was made by Burggraf [26] to numerically substantiate the indicated hypothesis for a square cavity; however, at that time, the methodical and computational limitations prevented obtaining of an acceptable result. In the comparatively recent works [4, 5, 9, 20], results of calculations of a stationary circulation flow in a square cavity with a moving cover at large Reynolds numbers (of the order of $5 \cdot 10^4$) were analyzed. It has been shown that, as Re increases, the solution of the problem becomes asymptotical in character, the stream-function modulus (the flow rate of the primary large-scale vortex) reaches a maximum gradually, and a vortex pattern with a central primary vortex, an angular secondary vortex, and a tertiary vortex is stabilized. Thus, in a

square cavity there arises not a single vortex, as Batchelor thought, but different-scale vortices with constant-vorticity cores surrounded by shear layers, i.e., the Batchelor hypothesis is only acceptable partially.

In the present work, attention is focused on the analysis of the solutions of the Navier–Stokes equations for the circulation flow of an incompressible viscous fluid in a square cavity with a moving cover at a moderate Reynolds number $Re = 10^3$, obtained with account for the structure of the primary vortex with a constant-vorticity core and a surrounding shear layer.

Evolution of the Computational Algorithm. The principal positions of the methodology of solving problems of aerohydraulics and heat exchange, realized in the modern package technologies, were developed in the 1980s [21, 22]. The Navier–Stokes equations were usually represented in natural variables and a centered template was selected for calculation of flows in complex-topology objects because these calculations call for the use of oblique meshes. The indicated equations were digitized by the finite-volume method with representation of convective and diffusion flows by schemes of not less than second order of approximation as a rule to avoid the distorting influence of the numerical diffusion. The algorithm of solving the initial equations was constructed within the framework of the concept of splitting by physical processes with the use of the SIMPLEC procedure of pressure correction involving the replacement of the continuity equation by the equation of pressure correction. The coordination of the velocity and pressure fields calculated with the use of a centered mesh was performed by the Rhie–Chow method involving the correction of the mass flows through the faces of the cells in the process of determining the pressure correction [27].

The computational methodology realized in the programs and forerunners of the VP2/3 package is similar on the whole to the methodology realized in the modern VP2/3-package versions; however, it has original features [23]. Unlike the methods of [23, 29–31], in the indicated methodology, the system of initial equations is written in the delta-form in the curvilinear coordinates consistent with the boundaries of the computational region relative to the increments of the dependent variables [22, 28]. The linearized system of initial equations is solved using a consistent SIMPLEC finite-volume procedure of pressure correction. For decreasing the numerical diffusion in the calculations of separation flows, in particular those that are sensitive to the errors in the approximation of the convective members of the transfer equations, in the explicit side of the motion equations, a one-dimensional analog of Leonard’s upwind scheme with quadratic interpolation (the QUICK scheme) is used [19]. For prevention of spurious oscillations in the representation of flows with thin shear layers, in the implicit side of these equations, the mechanism of artificial diffusion is used in combination with one-side upwind differences for representation of convective numbers. For elimination of the nonmonotonicity of the pressure field in the digitization of the pressure gradient by a central-difference scheme with the use of a centered template, a Rhie–Chow monotoner [27] with an empirical multiplier of 0.1, determined in the numerical experiments on the flows about a cylinder and a sphere, is introduced into the pressure-correction unit [28]. The high efficiency of the computational procedure for solving discrete algebraic equations is provided with the use of the incomplete matrix factorization method in the Stone SIP version [32]. An important element of the methodology developed in [28] is the introduction of the Rhie–Chow monotoner only at the stage of calculating the defect of the mass of a cell in the pressure-correction unit; this monotoner is not used in solving the momentum equations. Such an approach was used at a later time in the development of the generalized pressure-correction method for calculating incompressible and compressible fluid flows [2, 5, 8]. In [33], this approach was called the implicit method of using the Rhie–Chow correction.

The above-described algorithm of calculating nonstationary fluid flows is difficult to realize because it involves a passage from one time step to another, which disturbs the pressure fields. This is explained by the fact that, in the standard approach [28], the contribution of the Rhie–Chow monotoner to the total flow at the face of a cell is dependent on the empirically determined coefficient independent of the other parameters of the scheme used, such as the relaxation coefficient in the dynamic equation and the time step. The undesirable effect becomes especially obvious in the case where a small time step is used, and, consequently, the Rhie–Chow correction has practically no influence on the computational process. The generalization of the Rhie–Chow approach made in [35] makes it possible to obviate the above indicated differences. Two main features should be considered. First, the flows calculated with the use of the Rhie–Chow monotoner not only are used in the pressure-correction equations, but also are stored and then used for simulation of convective terms in all the transfer equations (of turbine, energy, concentration, and others). Thus, one more stage — the calculation of the flows at the faces of a cell — appears in the numerical procedure. This calculation is carried out after the solution of the dynamic equation before the pressure-correction stage. After the pressure correction is determined, not only the velocities of the flows at the centers of the cells, but also the normal components of this velocity at their faces, i.e., the values of the mass flows, are corrected. The second feature is even more important. It consists of the fact that the normal component of the flow velocity at the face of a

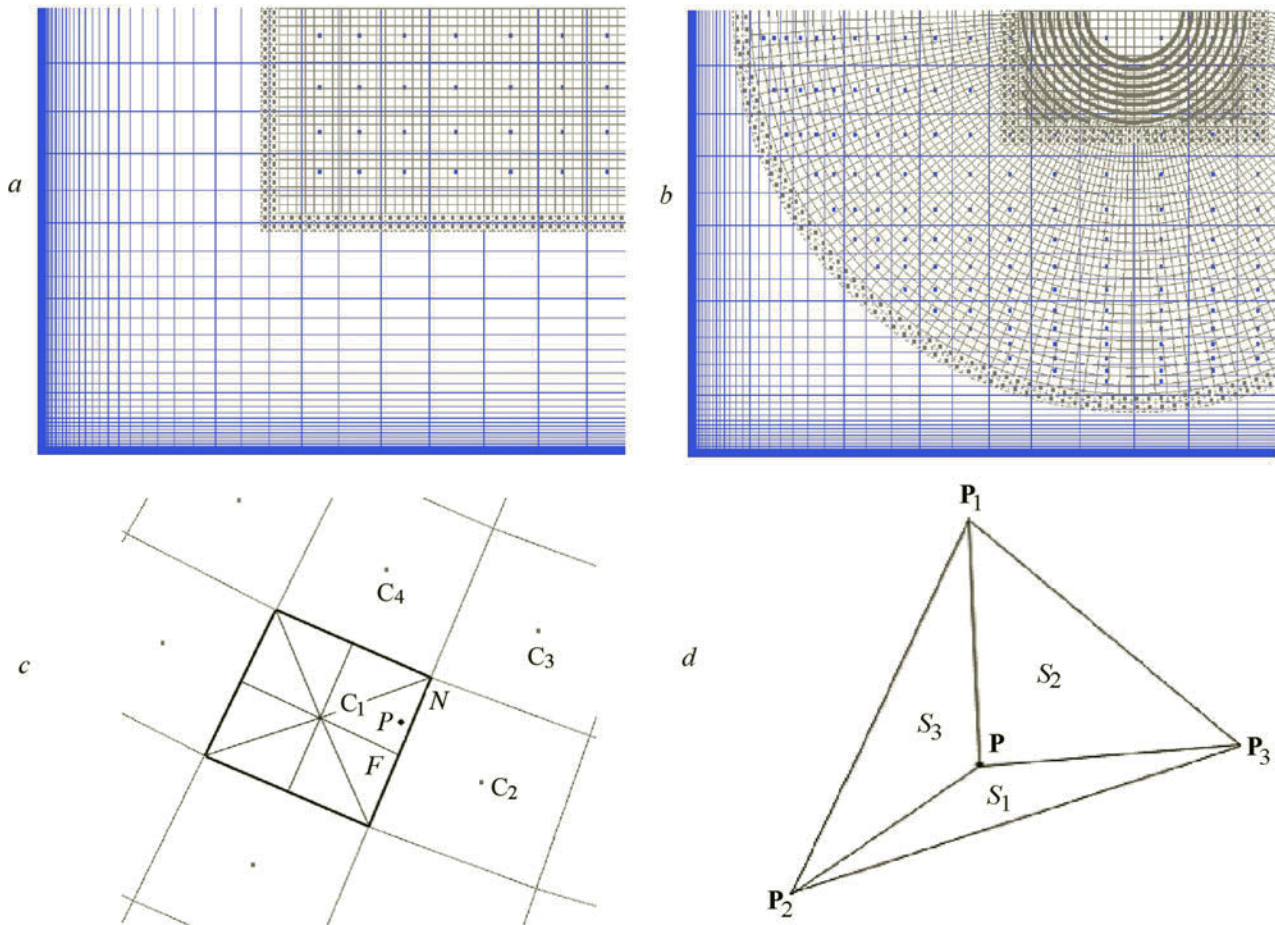


Fig. 1. Typical composite meshes of the H (a) and O (b) types with marked centers of the connected cells and schemes of intermesh interpolation: c) disposition of the point P of a connected cell of the internal mesh on the external mesh; d) determination of a parameter at this point by its values at the corners of the corresponding triangle.

cell is determined by not the simple averaging of the flow-velocity values, as in [28], but by the averaging of the flow-velocity values obtained from the discrete dynamic equations for the adjacent cells. This allows one, in the determination of the normal component of the flow velocity at the face of a cell, to distinctly separate the flow components proportional to the value of this velocity at the previous iteration and the previous step, to determine the dependence of these components on the mass forces, and to introduce, into the determination of the flow velocity, the local value of the normal component of the pressure gradient calculated only by its values in the adjacent cells. In this approach, the Rhie–Chow monotimizer appears automatically with a coefficient equal to the relaxation coefficient of the dynamic equation. Since the value of the flow at the previous iteration (previous time step) is present in the current value of the flow at the face of the cell, a change in the flow parameters does not cause a sharp increase in the errors. Moreover, it can be shown that the converged solution (if it exists) is independent of these parameters. An analogous approach, with the obvious use of the Rhie–Chow correction, was used in [33].

We call the reader's attention to an important aspect associated with the writing of the above-described algorithm simultaneously for structured and nonstructured grids (this problem was partially considered in [5]).

As already noted, multiblock computational technologies were developed for calculating flows in multiconnected regions with the use of composite grids superimposed on each other with intersection (overlapping grids) [4, 6–8]. An important element of the algorithm being considered is the intermesh interpolation of the dependent variables from one mesh to another. We will illustrate this interpolation by the example of solving the problem being investigated. As in [3, 4], all the cells of a composite mesh are divided into two groups: the computational cells, in which the initial equations are solved, and the connected cells, in which the parameters of the flow are determined by the intermesh interpolation. Figure 1a and b shows

composite meshes of two types: the meshes including an internal Cartesian mesh in the square subregion (Fig. 1a) and a set of internal meshes including a cylindrical mesh in the ring subregion and a Cartesian mesh in the square "patch" (Fig. 1b). In Fig. 1a and b, the heavy square points represent the centers of the connected cells.

At the preliminary stage of calculations, a minimum bounding rectangle is determined for each computational cell of the mesh (Fig. 1c), and an R* tree is constructed on the basis of these rectangles [34], which allows one to rapidly find the cell, in which a definite point representing a center of a connected cells of the internal mesh is found. From the R* a cell or a set of cells, the minimum bounding rectangles of which include a given point, is determined. Then the cells from this set are divided into the triangles, each of which is constructed at the center of a cell, at the center of its face, and at a corner point of the cell. The total number of these triangles will be equal to the twice the number of the faces of the cell.

Considering successively all the triangles, we find the triangle for which the barycentric coordinates of the given point are nonnegative, i.e., inside which this point is found (the triangle with the vertices C_1FN in Fig. 1).

The value of the flow at the vertex of the cell C_1 is equal to the value of the flow at the center of the cell, which is known. The value of the flow at the vertex F (the center of the cell face) is determined by the values of the flow in the cells C_1 and C_2 , weighted with account for the distances along the normal from the centers of the cells to their faces. The value of the flow at the vertex N is determined by averaging its values in all the cells, for which the vertex N is common, i.e., in the cells C_1-C_4 for the case being considered.

The interpolation dependence inside the triangle in Fig. 1d is written in barycentric coordinates: $V = \sum_1^3 h_i V_i$, where V_i is the velocity of the flow at the i th node of the mesh.

The weight coefficients h_i for an arbitrary triangle are determined from the following ratios:

$$h_1 = S_1/S, \quad h_2 = S_2/S, \quad h_3 = S_3/S.$$

Here S is the whole area of the triangle, and the inner areas S_i are calculated as a z coordinate of the vector product, e.g., $S_1 = \frac{1}{2}((\mathbf{P}_3 - \mathbf{P}_2)(\mathbf{P} - \mathbf{P}_2))_z$; therefore, the coordinates of a point can be negative when it is found outside the triangle.

It should be noted that the above-described procedure imposes no restrictions on the shape of a mesh cells and, consequently, can be realized with the use of both structured and nonstructured meshes.

Modifications of the VP2/3 Package. Modern program packages used for engineering analysis have a module structure and include a preprocessor (a unit for preparation of initial data), a solver (the core of a package with a catalog of mathematical models), and a postprocessor (an interpreter of the calculation data obtained). The predecessors of the VP2/3 package are programs written on the algorithmic Fortran-77 language [22]. The emphasis shown by researchers on the graphical processing of calculation data, including the monitoring of the computational process in the representation of the behavior of the trajectories error in the special window, resulted in the use of not the most efficient program-oriented DELPHI medium [4]. It is significant that multiblock computational technologies were realized in the single-processor version of the VP2/3 package. For the unparallelization of this package, the initial codes were rewritten in C++. At the final stage of the development of the VP2/3 package, it was substantially modified with the use of the coordinated computational procedure, which can be realized with both the structured and nonstructured meshes.

Comparison of the Results of Numerical Calculations Obtained with the Use of Different-Density Multiblock Meshes and Different Versions of the VP2/3 Package. The above consideration of the development of package technologies is a continuation of the methodological investigation carried out in [9, 10]. The results of an investigation of the influence of the density of an $N \times N$ mesh and its near-wall step δ_m on the convergence of the iteration process and the accuracy of calculating the integral and extremum local characteristics of the flow in a square cavity with the use of different versions of the VP2/3 package are presented in Figs. 2 and 3, and in Table 1. In the solution of such problems, as an initial approximation, a Reynolds number of 10^2 is used, or the fields of dependent variables calculated at $Re = 10^3$ are reinterpolated on a coarse mesh.

The convergence trajectories were determined by the behavior of the errors in determining the longitudinal component of the flow velocity $ErrU$ and the pressure $ErrP$ (pressure correction), i.e., the increments in the dependent variables at each iteration step, and of the scaled errors (scaled residuals), in particular $ErrUnr$ [5], which are widely used in the Fluent, CFX, StarCD, and other packages. First and foremost, the fairly slow convergence of the computational process in solving the problem being considered, i.e., the attainment of the given level of increments equal to 10^{-7} with the use of about 10,000 iterations, has attracted our attention. In this case, the normalized error is smaller by an order of magnitude as compared to the

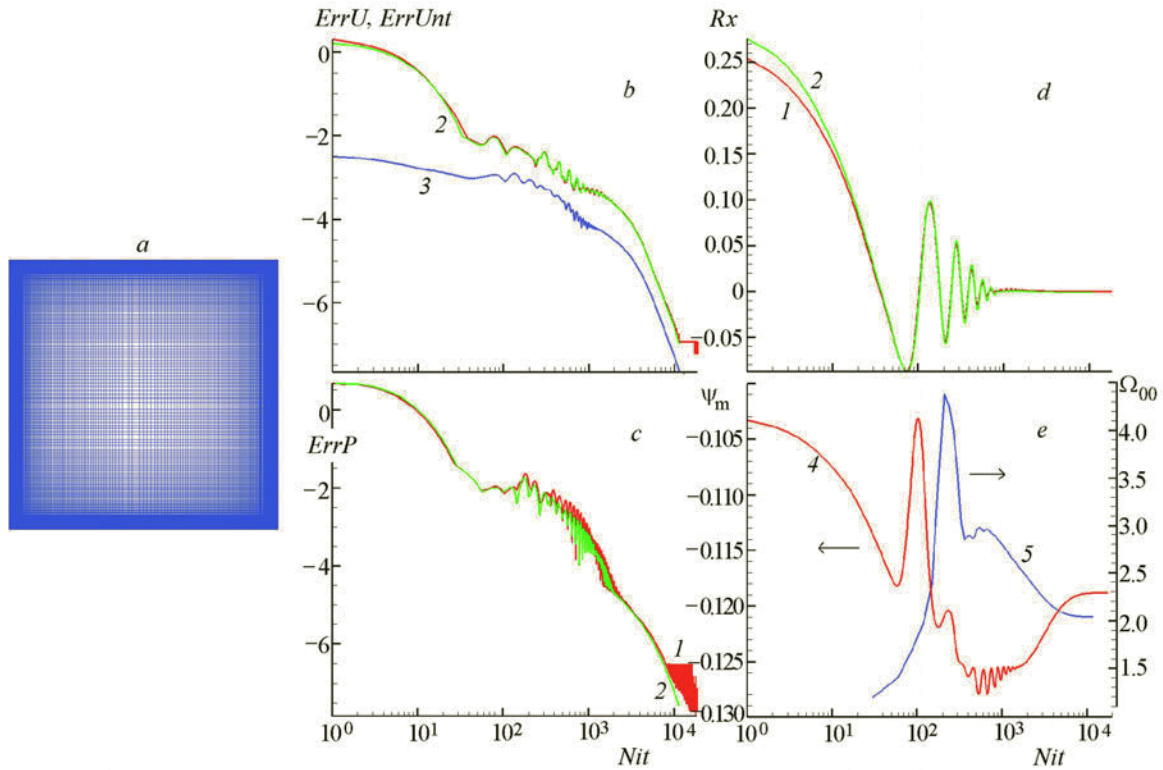


Fig. 2. Mesh of size 200×200 with a near-wall step of 10^{-3} (a), comparison of the trajectories of the errors in determining the longitudinal component of the flow velocity $ErrU(Nit)$ and of the scaled error $ErrUnr(Nit)$ (b), behavior of the pressure correction $ErrP(Nit)$ (c), comparison of the integral force loads on the walls of the cavity $R_x(Nit)$ (d), and dependences of the minimum stream function $\psi_m(Nit)$ and the vortex at the center of the cavity $\Omega_{00}(Nit)$ on the parameter Nit (e): 1, 4, 5) DELPHI version of the VP2/3 package; 2, 3) C++ version of the VP2/3 package. The solutions at $Re = 10^2$ were used as initial approximations.

ordinary increments (Fig. 2b), which creates the illusion of attainment of convergence of the problem even though it has yet to be solved. This feature of the problem on the circulation flow in a cavity was considered in [10]. It was established that, in addition to the monitoring of the behavior of the errors, it is necessary to control the integral characteristics. It was proposed in [22] to use, as an indicating characteristic, the maximum (in absolute value) stream function in the cavity, corresponding to the rate of the fluid flow in the primary vortex, which is accelerated by the movement of the cover. In the present investigation, we additionally controlled the behavior of the longitudinal resistance force R_x acting on the cavity walls. One more interesting conclusion follows from the analysis of the data presented on Table 1. The value of the criterion determining the completion of the iterations influences the solution of the problem. It is usually assumed that $ErrU_0 = 10^{-5}$ [9, 10]. However, it follows from Table 1 that $ErrU_0$ should be equal to 10^{-7} .

Figure 2 shows estimates made with the use of the old VP2/3 package written in DELPHI and estimates made with the use of the new VP2/3 package, whose unparallelization codes are written in C++. In Table 1, the calculation data obtained by the methodology of [22, 28] and by the consistent methodology described in the present work are given. It should be noted that the numerical data presented in Fig. 2, which were obtained with the use of different versions of the VP2/3 package, are in good agreement. The marked deviation of the total number of iterations before the convergence of the solution obtained using the DELPHI version of the package VP2/3 from that obtained with the use of the C++ version is probably explained by the fact that the old VP2/3 package was developed for a 32-bit operating system. Moreover, in the new C++ version of this package, nonstructured meshes are used and, therefore, the upwind schemes of the second and higher orders can give different results on nonuniform meshes.

TABLE 1. Influence of the Step (the number of cells) of a Mesh at the Center of the Computational Region and the Near-Wall Step on the Extremum Characteristics of the Circulation Flow in the Square Cavity with a Moving Cover at a Constant Reynolds Number of 10^3

| N | δ_m/δ_{\max} | $-\psi_m$ | $-u_m$ | $-v_m$ | v_{\max} | $-10^3 f_m$ | Ω_{00} |
|-----------|--------------------------|-----------|--------|--------|------------|-------------|---------------|
| 200*** | $10^{-3}/0.142$ | 0.1187 | 0.3895 | 0.6796 | 0.3816 | 4.049 | 2.056 |
| 200 ** | $10^{-3}/0.142$ | 0.1188 | 0.3899 | 0.6797 | 0.3826 | 4.049 | 2.049 |
| 200 old** | $10^{-3}/0.142$ | 0.1889 | 0.3900 | 0.6797 | 0.3827 | 4.221 | 2.050 |
| 200 del** | $10^{-3}/0.142$ | 0.1188 | 0.3899 | 0.6797 | 0.3827 | 4.231 | 2.049 |
| 400*** | $10^{-4}/0.0121$ | 0.1187 | 0.3897 | 0.6797 | 0.3820 | 4.066 | – |
| 400 ** | $10^{-4}/0.0121$ | 0.1189 | 0.3902 | 0.6799 | 0.3828 | 4.122 | 2.051 |
| 400 | $10^{-4}/0.0121$ | 0.1188 | 0.3901 | 0.6799 | 0.3827 | 4.237 | 2.049 |
| 400*** | $5 \cdot 10^{-4}/0.0071$ | 0.1187 | 0.3895 | 0.6794 | 0.3816 | 4.059 | 2.063 |
| 400 ** | $5 \cdot 10^{-4}/0.0071$ | 0.1189 | 0.3903 | 0.6799 | 0.3828 | 4.059 | 2.059 |
| 400 ** | $10^{-3}/0.005$ | 0.1189 | 0.3902 | 0.6797 | 0.3828 | 4.210 | 2.059 |
| 1000 | 10^{-3} | 0.1189 | 0.3903 | 0.6797 | 0.3828 | 4.214 | 2.065 |

Note. The errors in determining the flow-velocity components $ErrU_0$ is 10^{-7} ; *) $ErrU_0 = 10^{-5}$; **) 32-bit system; old) C++ version (the calculation begins with $Re = 100$, $Nit = 11,000$); del) DELPHI version (the calculation begins with $Re = 100$, $Nit = 18,500$).

An analysis of the behavior of the integral and local parameters R_x , ψ_m , and Ω_{00} has shown that the change in them at the initial stage of the convergence process is pulsating rather than monotonic in character within the first thousand of iterations (Fig. 2d and e). In this case, the errors reach 10^{-4} – 10^{-3} and the integral force load is stabilized. However, at this stage, the solution of the problem is still far from completion and, in the subsequent 900 iterations, ψ_m monotonically increases and Ω_{00} at the center of the cavity gradually decreases and attains an asymptotic value.

The influence of the density of a multiblock mesh with a fairly small near-wall step (10^{-4}) on the convergence of the iteration solution is illustrated in Fig. 3. It is seen that a change in the mesh density leads to a large change in the total number of iterations (by 10 times, from 2 to 20 ths) until the solution of the problem is completed. In this case, the number of cells in the cavity increases from 10 to 160 ths, i.e., by 16 times.

Comparison of the Results of Calculations of the Circulation Flow in a Square Cavity with the Use of Different-Topology Meshes Including Composite Ones and Analysis of the Applicability of MCTs. Some results of our methodical investigation are presented in Figs. 3–9 and in Table 2.

Composite meshes were generated by imposition of uniform square and ring meshes on the nonuniform Cartesian meshes that are usually used in the calculations of a circulation flow of an incompressible viscous fluid in a square cavity with a moving cover. The superimposed meshes were symmetrical relative to the walls of the cavity. In the case where an O-type mesh was used, a square "patch" with square cells was superimposed on the central zone. In principle, the use of a multiblock computational technology for solving the problem of flow in such a cavity is not seen as necessary, unlike the situation with multiconnected subregions where the usual approaches obviously cause complications and lead to a decrease in the accuracy of numerical estimations. However, in addition to the monitoring of the errors introduced by multiblock computational technologies in calculations and the comparison of the superimposed different-type meshes, it is useful to estimate the influence of them on the efficiency of the calculations carried out with the use of moderate-resource computers. It is advantageous to use composite meshes with cells decreasing substantially as the wall of the cavity is approached (with a step of the order of 10^{-4} at high Reynolds numbers), which provides a proper resolution of the structural elements of the flow at a large distance from the cavity wall. Multiblock meshes, including nonstructured ones, are usually designed for representation of complex-geometry streamlined surfaces and the structure of the flow near the wall of a cavity without regard

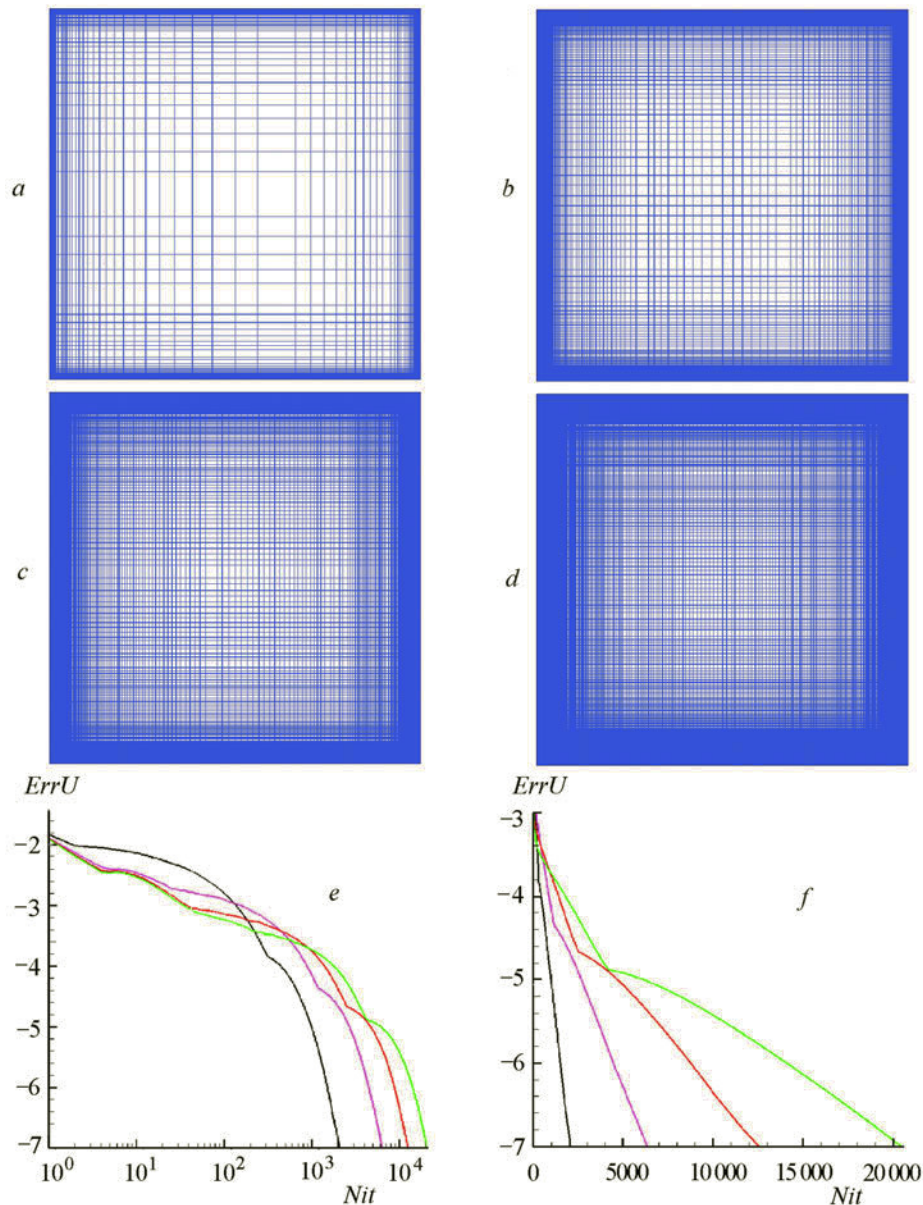


Fig. 3. Different-density multiblock computational meshes of size 100×100 (a), 200×200 (b), 300×300 (c), and 400×400 (d) with a constant near-wall step and convergence trajectories in the logarithmic (e) and linear (f) scales. The solutions at $Re = 10^2$ were used as initial approximations.

for the character of the flow at a large distance from the cavity wall where the sizes of the computational cells are comparable or exceed the characteristic scales of the flow elements. In the case where moderate multiblock meshes (Fig. 2) with a small near-wall step (10^{-4}) are used, the size of the computational cell at the center of the cavity is extremely large to provide an exact representation of the core of the primary vortex. By this reason, it is necessary to cover this zone by an additional fine mesh of the H or O type, and the latter topology of the mesh agrees with the character of the circulation flow in the cavity. A systematic investigation should begin with the determination of the influence of the dimension of the inner square region divided by a square mesh with a step of 0.01 on the process being considered. The size of the superimposed mesh varies from 0.4 to 0.95, and the external mesh consistent with the walls of the cavity contains 100×100 cells with a near-wall step of 10^{-4} . At the second stage of the investigation, emphasis should be laid on the variation of the density of the external mesh on condition that the size of the internal square mesh (0.95×0.95) divided into 100×100 square cells remains unchanged.

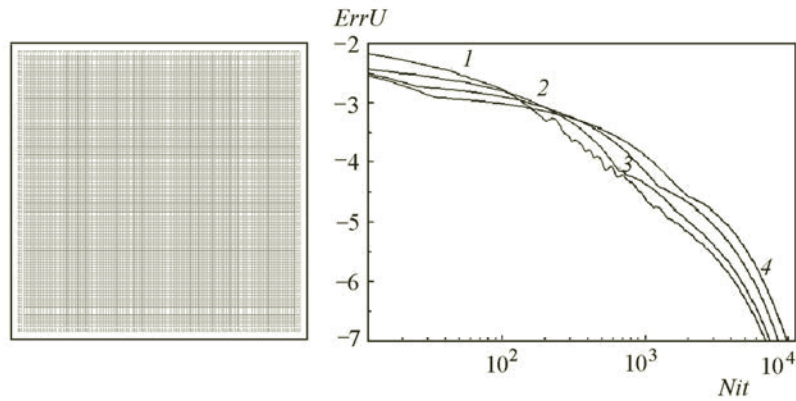


Fig. 4. Convergence trajectories in the calculations with the use of composite meshes including a constant internal uniform 100×100 mesh covering the square region of size 0.95×0.95 and internal meshes with $N = 100$ (1), 150 (2), 200 (3), and 250 (4). The solutions at $Re = 10^2$ were used as initial approximations.

TABLE 2. Influence of the Type of a Composite Mesh on the Extremum Characteristics of the Circulation Flow in the Square Cavity with a Moving Cover at a Constant Reynolds Number of 10^3

| Basic mesh | NN | Additional mesh, δ_m/δ_{max} | $-\psi_m$ | $-u_m$ | $-v_m$ | v_{max} | $-10^3 f_m$ | Ω_{00} |
|--------------------------------|----------------|--|-----------|--------|--------|-----------|-------------|---------------|
| <i>Multiblock meshes</i> | | | | | | | | |
| 1 | 10^4 | $10^{-4}/0.0615$ | 0.1145 | 0.375 | 0.6797 | 0.3700 | 4.500 | 1.866 |
| 2 | $4 \cdot 10^4$ | $10^{-4}/0.0278$ | 0.1185 | 0.389 | 0.6798 | 0.3818 | 4.257 | 2.031 |
| 3 | 10^7 | 10^{-3} | 0.1189 | 0.3903 | 0.6797 | 0.3828 | 4.214 | 2.065 |
| <i>Composite O-type meshes</i> | | | | | | | | |
| 1 | 16,090 | Ring 41×201 mesh | 0.1170 | 0.3843 | 0.6799 | 0.3776 | 4.473 | 2.015 |
| 2 | 44,260 | | 0.1181 | 0.3876 | 0.6799 | 0.3804 | 4.256 | 2.043 |
| <i>Composite H-type meshes</i> | | | | | | | | |
| 1 | 16,612 | 90×90 mesh with a step of 0.01 | 0.1176 | 0.3865 | 0.6793 | 0.3789 | 4.363 | 2.041 |
| 2 | 42,160 | 95×95 mesh with a step of 0.01 | 0.1187 | 0.3892 | 0.6811 | 0.3823 | 4.142 | 2.064 |
| 1 | 11,716 | 50×50 mesh in the region of size 0.8×0.8 | 0.1156 | 0.3793 | 0.6800 | 0.3720 | 4.416 | 1.995 |
| 1 | 18,732 | 100×100 mesh in the region of size 0.8×0.8 | 0.1158 | 0.3806 | 0.6795 | 0.3733 | 4.452 | 1.995 |
| 1 | 17,920 | 100×100 mesh in the region of size 0.95×0.95 | 0.1178 | 0.3871 | 0.6795 | 0.3795 | 4.254 | 2.048 |
| 2 | 46,716 | 100×100 mesh in the region of size 0.8×0.8 | 0.1181 | 0.3874 | 0.6798 | 0.3800 | 4.282 | 2.046 |

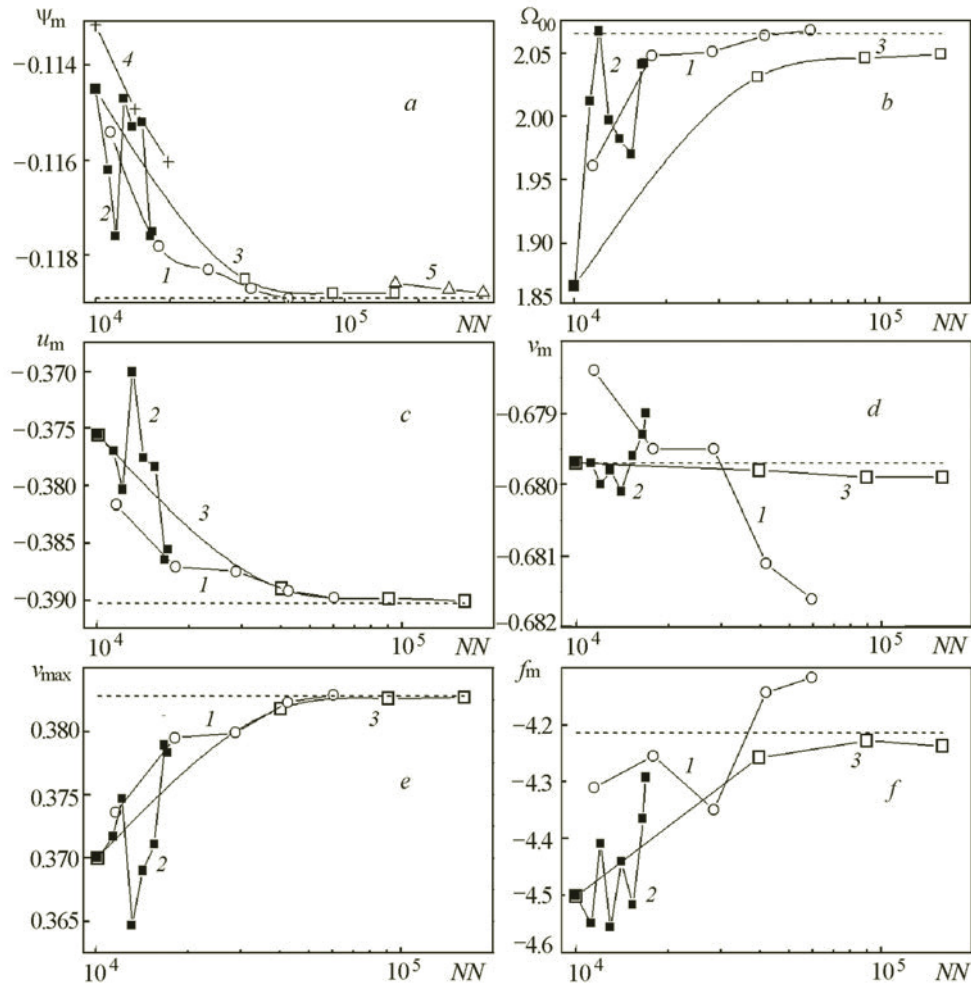


Fig. 5. Dependences of ψ_m (a), Ω_{00} (b), u_m (c), v_m (d), v_{\max} (e), and f_m (f) on the total number of computational cells $N \times N$: 1) multiblock meshes with $\delta_m = 10^{-4}$; 2) composite mesh including an external 100×100 mesh with $\delta_m = 10^{-4}$ and internal square meshes with $\delta_m = 10^{-2}$ and sizes changing from 0.4 to 0.9 with a step of 0.1; 3) composite mesh including a constant internal 100×100 mesh in the subregion of size 0.95×0.95 and an external mesh with N changing from 50 to 250 with a step of 50 cells at $\delta_m = 10^{-4}$; 4) data of [36]; 5) data of [20]. The dashed lines represent the asymptotic values obtained with the use of a uniform $10^3 \times 10^3$ mesh.

At $\delta_m = 10^{-4}$, N changes from 100 to 250 with a step of 50. The trajectories of convergence of the calculation carried out with the use of such composite meshes (Fig. 4) differ insignificantly from each other (the number of iterations necessary for the convergence of the solution falls within the range 7–10 ths) even though the total number of the computational cells NN changes markedly (from 18 to 60 ths). The influence of NN of the composite and multiblock meshes on the local and integral characteristics of the flow in the square cavity is demonstrated in Fig. 5.

As NN increases, the minimum value of the stream function in the cavity, characterizing the flow rate of the fluid involved in the large-scale vortex motion, gradually approaches the asymptotic level (Fig. 5a). It is apparent that composite meshes introduce systematic errors into the results of calculations due to the intermesh interpolation. The maximum error in determining ψ_m is of the order of 3.5% in the case where ψ_m changes nonmonotonically depending on NN (curve 2) with change in the size of the additional square mesh. At the same time, the use of a composite mesh including a square mesh of size 0.95×0.95 in the process of successive refinement of the near-wall zone (curve 1) makes the solution more exact as compared to that obtained with the use of the basic multiblock mesh (curve 3). For comparison, Figure 5a presents the

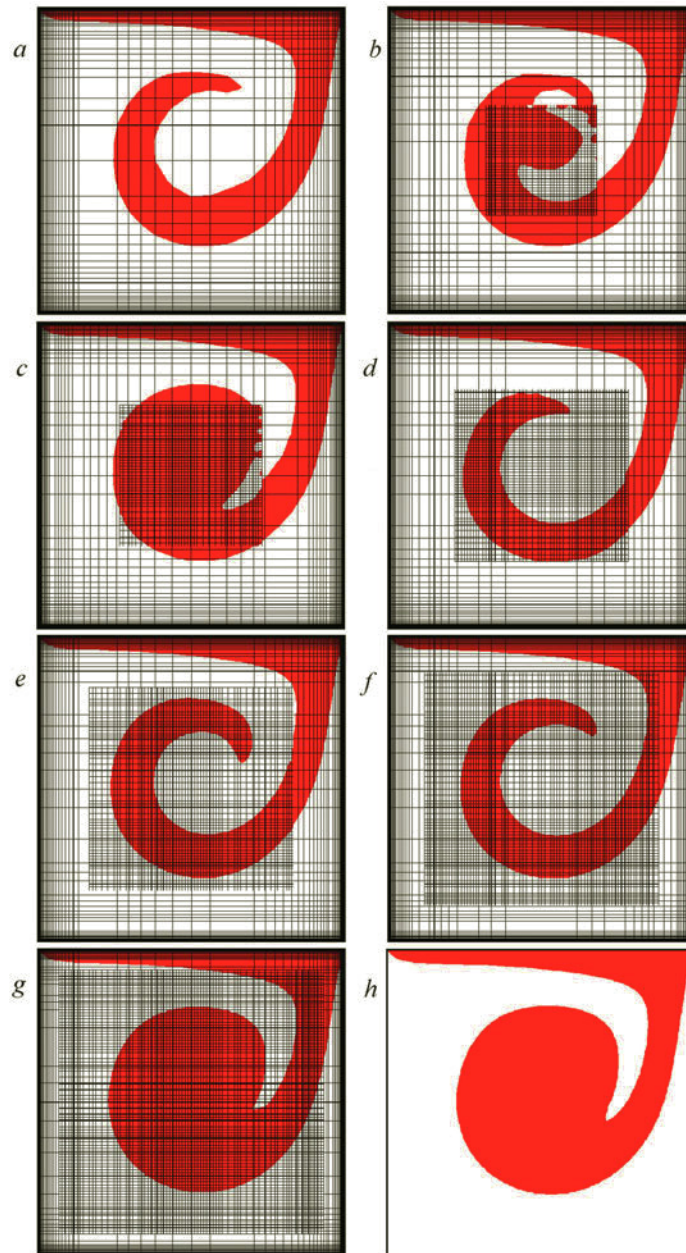


Fig. 6. Comparison of the zones $\Omega = 2$ represented on the initial multiblock 100×100 mesh with $\delta_m = 10^{-4}$ (a) and on the composite meshes including additional internal square meshes with $\delta_m = 10^{-2}$ and subregions of size 0.4×0.4 (b), 0.5×0.5 (c), 0.6×0.6 (d), 0.7×0.7 (e), 0.8×0.8 (f), and 0.9×0.9 (g) and the zone Ω obtained using a 400×400 mesh with $\delta_m = 10^{-4}$ (h).

solutions of the Navier–Stokes equations in the transformed variables [20, 36]. It should be noted that the most recent of them have been obtained with the use of fourth-order schemes and very fine meshes, and they are exceeded by the solutions obtained in the present work.

It follows from Fig. 5b that the estimates of Ω_{00} made with the use of moderate composite meshes are more exact than those obtained with the use of multiblock meshes. The maximum error in determining the maximum velocity of the backflow u_m with the use of a composite mesh including a variable square mesh (curve 2, Fig. 5c), equal to 7.5%, seems large too. However, the estimates made with the use of moderate-resource composite meshes including a constant subregion of size

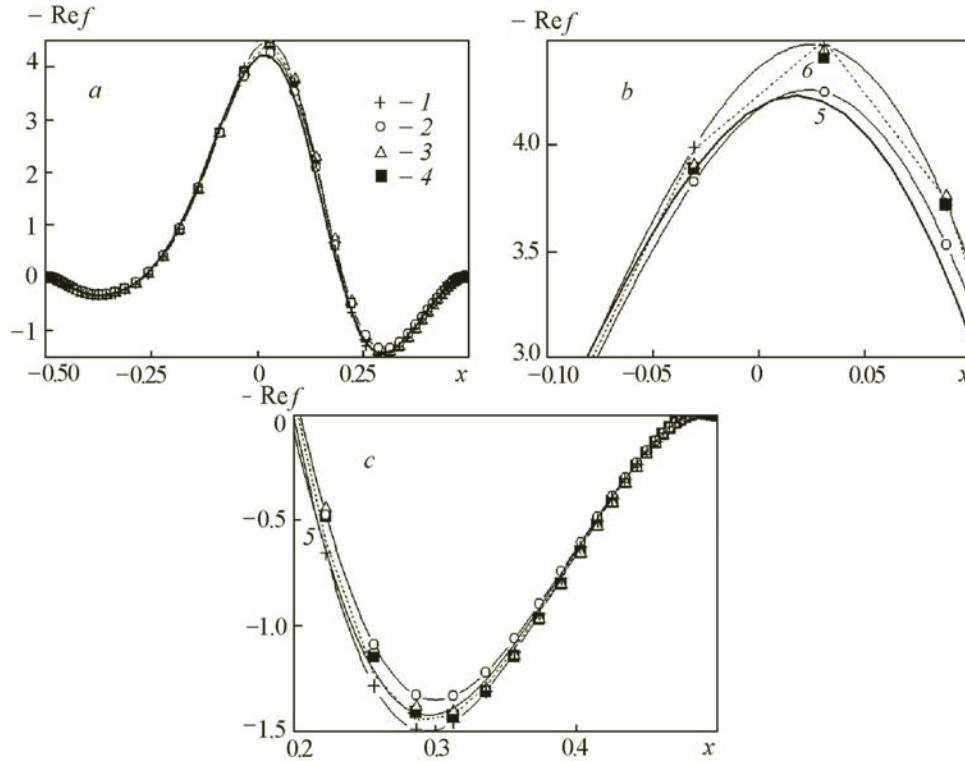


Fig. 7. Comparison of the friction distributions at the bottom of the cavity calculated using composite meshes including superimposed H- and O-type meshes (1–4), a standard 400×400 mesh (the full line 5), and a standard multiblock 100×100 mesh (the dashed line 6) with $\delta_m = 10^{-4}$: 1) ring mesh with a patch; 2) square 100×100 mesh with a subregion of size 0.95×0.95 ; 3) square 100×100 mesh with a subregion of size 0.8×0.8 ; 4) square 50×50 mesh with a subregion of size 0.8×0.8 .

0.95×0.95 (curve 1) are more exact than those made with the use of an analogous multiblock mesh (curve 3). The accuracy of estimation of v_m with the use of any mesh is acceptable (Fig. 5d), and the change in v_{\max} with increase in NN (Fig. 5e) is analogous to the behavior of the dependence $u_m(NN)$. The errors in determining the minimum friction at the bottom of the cavity with the use of composite meshes are of the same order or even somewhat smaller than those in the case of use of multiblock meshes (Fig. 5f); the maximum error is of the order of 5%.

The evolution of the zone $\Omega = 2$ (Fig. 6) calculated with the use of multiblock and composite meshes explains well the reason for the nonmonotonic behavior of the errors in determining ψ_m , u_m , and v_m in the case where the subregion occupied by the internal square mesh widens gradually. It is seen that the maximum errors are obtained in the case where the size of the subregion falls within the range 0.6–0.8 and the constant-vorticity spot is transformed into a protuberance.

Comparison of the friction distributions at the bottom of the cavity (Fig. 7), calculated with the use of composite meshes including superimposed meshes of the H and O types (1–4), a standard 400×400 mesh (the full line 5), and a basic multiblock 100×100 mesh (the dashed line 6) with $\delta_m = 10^{-4}$, shows that these distributions differ insignificantly from each other, even though the differences between the friction distributions at the central region of the cavity bottom are marked (Fig. 7b). The solutions obtained with the use of internal 50×50 (data 4) and 100×100 (data 3) square meshes including a subregion of size 0.8×0.8 agree well with the solution obtained with the use of a ring mesh (data 1). The solutions obtained for ψ_m with the use of meshes having close total numbers of cells NN are also in good agreement (approximately 0.116 and 0.117, Table 2). Thus, the step of an internal mesh $\delta = 0.02$ is entirely acceptable. It should be noted that the solutions obtained with the use of an internal 100×100 mesh including a subregion of size 0.95×0.95 are practically identical to the solutions obtained with a standard multiblock 400×400 mesh.

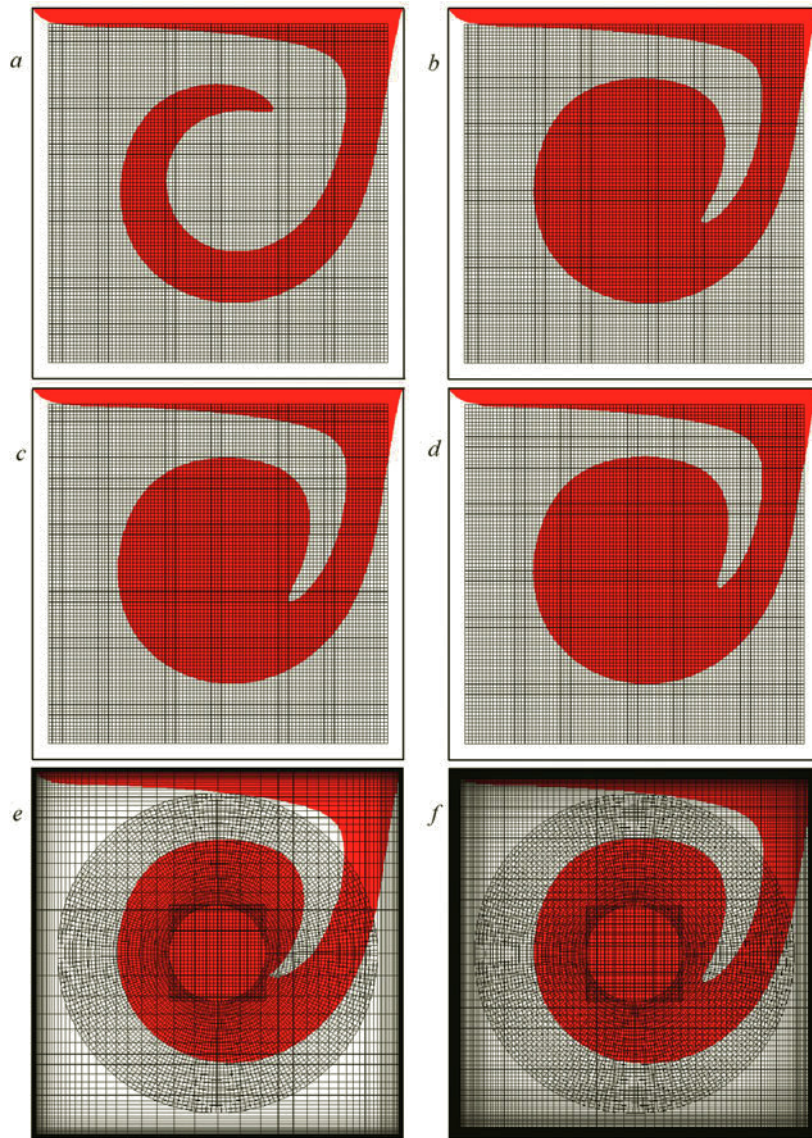


Fig. 8. Comparison of the zones $\Omega = 2$ represented on the composite meshes including constant internal uniform H- and O-type meshes and varying external basic meshes with $\delta_m = 10^{-4}$: a) $N = 50$; b) $N = 100$; c) $N = 150$; d) $N = 200$ (a square 100×100 mesh covers the zone of size 0.95×0.95); e) $N = 100$; f) $N = 200$ (a ring mesh with a patch).

The evolution of the zone $\Omega = 2$ (Fig. 8) calculated with the use of the composite mesh including a constant square zone of size 0.95×0.95 and an external mesh with an increasing number of cells and $\delta_m = 10^{-4}$ shows that the core of constant vorticity is well estimated even with the use of an external 100×100 mesh. An entirely acceptable solution is obtained with the use of ring meshes too. Comparison of the local and integral characteristics of the flow being investigated, calculated with the use of different-topology composite meshes with approximately equal numbers of cells, show that these characteristics agree well.

When the friction distributions at the bottom of the cavity, calculated with the use of composite meshes including constant internal uniform meshes of the O and H type and nonuniform basic external meshes, are compared, it is apparent that they are estimated with an acceptable accuracy in the case where $N \geq 100$ (Fig. 9). Note that the introduction of an internal 100×100 square mesh covering the region of size 0.95×0.95 improves, by and large, the solution of the problem; however, as the external mesh is detailed beginning with $N = 200$, a small disagreement (curve 4) with the standard solution arises.

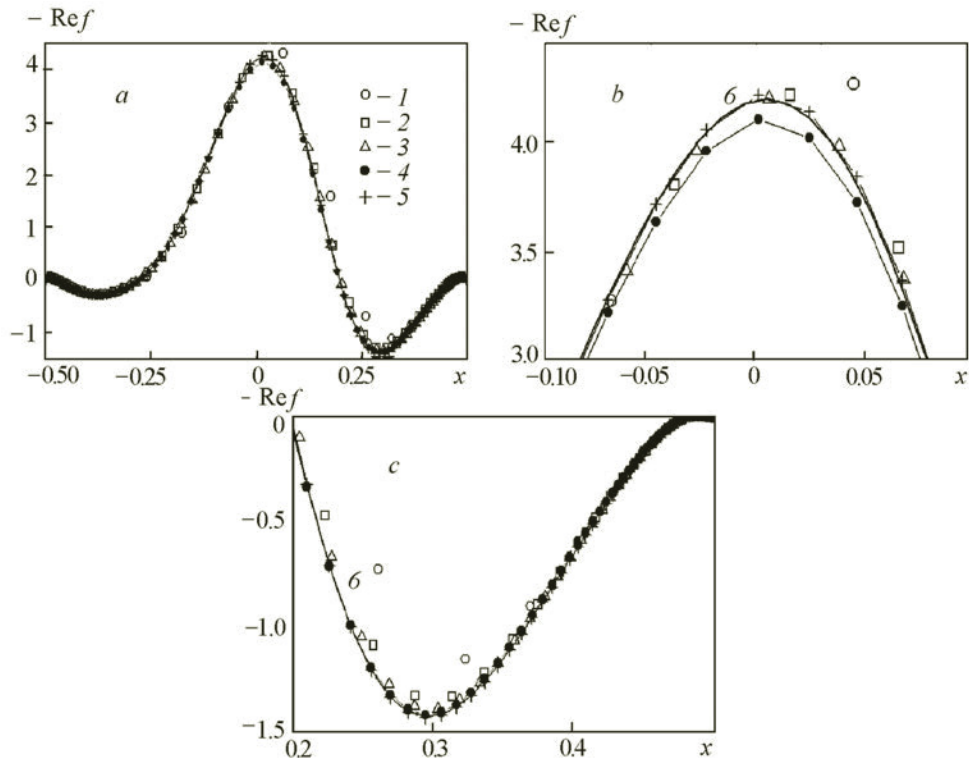


Fig. 9. Comparison of the friction distributions at the bottom of the cavity calculated using composite meshes including constant internal uniform meshes of the H and O types and varying external basic meshes with $\delta_m = 10$ and $N = 50$ (1), 100 (2), 150 (3), 200 (a square 100×100 mesh covers the zone of size 0.95×0.95) (4), 200 (a ring mesh with a patch) (5), and 400 (a standard multiblock mesh) (a, b) and fragment of the first-mentioned graph (c).

The below conclusions on the applicability of multiblock computational technologies for solving problems of aerohydrodynamics and heat exchange were made on the basis of the analysis of the influence of the density of multiblock and composite meshes, the topology of the superimposed meshes, the linear interpolation, and different versions of the VP2/3 package based on the SIMPLEC pressure-correction procedure on the solution of the test problem on the circulation flow of an incompressible viscous liquid in a square cavity with a moving cover.

CONCLUSIONS

1) The selection of the criterion $ErrU_0$ determining the completion of the iteration procedure influences the solution of the problem on the circulation flow of an incompressible viscous liquid in a square cavity with a moving cover. It has been established that the best value of this criterion is 10^{-7} and not 10^{-5} as it is usually taken.

2) Different versions of the VP2/3 package written in DELPHI and C++ give numerical estimations consistent in accuracy. The computational efficiency of the consistent Rhie–Chow method is half that of the method realized with the use of the Rhie–Chow monotonicizer in the explicit form with an empirically selected relaxation coefficient equal to 0.1.

3) The drag in a square cavity is stabilized in the nonmonotonic pulsed process approximately at the 1000th iteration, while the minimum stream function is attained and the vorticity is established at the center of the cavity during the additional 9000 iterations.

4) The 16-fold increase in the number of cells in a nonuniform Cartesian mesh with a constant near-wall step of 10^{-4} is accompanied by a 10-fold increase in the number of iterations until the computational process is converged.

5) A large increase in the total number of the computational cells in a composite mesh (from 18 to 60 ths) leads to a small increase in the number of iterations (from 7 to 10 ths).

6) The calculations carried out with the use of a composite mesh including a superimposed H-type mesh, a variable square subregion of size 0.4–0.9, a square mesh with a step of 0.01, and a constant internal 100×100 mesh with a near-wall step of 10^{-4} give nonmonotonic dependences of the minimum stream function, the minimum longitudinal velocity of the flow, and the maximum vertical velocity of the flow on the total number of the computational cells in the cavity; however, the maximum errors of the MCT in determining the indicated parameters, equal to 3.5%, 7.5%, and 4.5%, respectively, seem acceptable because a coarse basic external mesh was used in the calculations.

Unlike the indicated meshes, composite meshes including a constant internal subregion of size 0.95×0.95 divided by a 100×100 square mesh and a variable external mesh with a number of cells from 50×50 to 250×250 and a near-wall step of 10^{-4} refine the solution of the problem considered as compared to that obtained on the basic meshes with increasing densities and, especially, on those with moderate numbers of cells. At the same time, the basic meshes containing more than 200 cells give a small systematic error in determining the minimum friction at the bottom of the cavity.

7) The estimates made with the use of composite meshes of the H and O types with approximately equal numbers of computational cells are close in accuracy and computational efficiency.

8) A comparison of the results of the calculations carried out with the use of composite meshes with the standard solutions obtained with the use of limiting multiblock 400×400 and $10^3 \times 10^3$ meshes has substantiated the acceptability of the linear interpolation in the multiblock computational technologies, which was determined earlier in [4, 5].

The authors express their thanks to Professors V. M. Goloviznin and P. N. Vabishchevich for the very useful discussion of the computational methodology.

This work was carried out with financial support from the Russian Foundation for Basic Research (Projects Nos. 08-01-00059 and 12-08-90001).

NOTATION

$ErrU$ and $ErrP$, error in the longitudinal component of the flow velocity and pressure correction, in fractions of U and U^2 , respectively; $ErrUnr$, scaled error in the longitudinal component of the flow velocity, in fractions of U ; f , friction at the lower wall of the square cavity, in fractions of U^2 ; h , ratio between areas; L , size of a cavity face, m; N , number of cells on the cavity face; NN , total number of computational cells in the cavity; Nit , number of iteration steps necessary for the convergence of the computational process; \mathbf{P} , radius-vector determining the position of a point; $Re = UL/\nu$, Reynolds number; S , area, in fractions of L^2 ; U , velocity of movement of the upper cover, m/s; u and v , longitudinal and transverse velocities of the flow, in fractions of U ; x and z , longitudinal and transversal coordinates, in fractions of L ; R_x , total longitudinal force acting on the walls of the cavity, in fractions of U^2 and L ; V , variable at the mesh nodes; ν , kinematic viscosity coefficient, m^2/s ; Ω_{00} , vorticity at the center of the cavity, in fractions of U/L ; δ , size of the mesh step, in fractions of L ; ψ , stream function, in fractions of U and L . Subscripts: i , number of a mesh node; 0, minimum error in the completion of the iteration process; m, minimum; max, maximum.

REFERENCES

1. S. V. Guvernyuk, S. A. Isaev, A. G. Sudakov, et al., Multiblock computational technologies of solving the problems of aeromechanics and thermal physics, in: V. A. Sadovnichii, G. I. Savin, and V. V. Voevodin (Eds.), *Supercomputer Technologies in Science, Education, and Industry* [in Russian], Izd. MGU, Moscow (2012), pp. 198–203.
2. S. A. Isaev, A. G. Sudakov, P. A. Baranov, et al., Development, verification, and application of the open-type parallelized VP2/3 package based on the multiblock computational technologies for solving fundamental, applied, and operational problems of aeromechanics and thermal physics, *Vestn. Yuzhno-Uralsk. Gos. Univ., Ser. "Mat. Modelir. Programmir."*, No. 17 (150), Issue 3, 59–72 (2009).
3. P. A. Baranov, S. A. Isaev, Yu. S. Prigorodov, and A. G. Sudakov, Numerical simulation of a laminar flow around a cylinder with passive and active vortex cells within the framework of the concept of computational region decomposition and with the use of multistage meshes, *Pis'ma Zh. Tekh. Fiz.*, **24**, Issue 8, 33–41 (1998).
4. A. V. Ermishin and S. A. Isaev (Eds.), *Control of Flows around Bodies with Vortex Cells as Applied to Integrally Assembled Flying Vehicles: Numerical and Physical Simulation* [in Russian], MGU, Moscow (2003).
5. Yu. A. Bystrov, S. A. Isaev, N. A. Kudryavtsev, and A. I. Leont'ev, *Numerical Simulation of the Vortex Intensification of the Heat Transfer in Tube Banks* [in Russian], Sudostroenie, St. Petersburg (2005).

6. N. A. Kudryavtsev, *Vortex Intensification of the Heat Transfer in Heat Exchanger Elements and Its Numerical Simulation*, Author's Abstract of Doctoral Dissertation (in Engineering), SPb GPU, St. Petersburg (2005).
7. V. B. Kharchenko, *Numerical Simulation of Separation Flows with Vortex and Jet Generators on the Bases of Multiblock Computational Technologies*, Author's Abstract of Doctoral Dissertation (in Engineering), SPb MG TU, St. Petersburg (2006).
8. A. E. Usachov, *Development and Verification of Multiblock Computational Technologies Realized in the VP2/3 Package with Applications to Fundamental and Applied Problems of Aeromechanics and Thermal Physics*, Author's Abstract of Doctoral Dissertation (in Engineering), IPM im. M. V. Keldysha RAN, Moscow (2013).
9. S. A. Isaev, A. G. Sudakov, N. N. Luchko, and T. V. Sidorovich, Numerical simulation of laminar circulation flow in a square cavity with a moving boundary at high Reynolds numbers, *Inzh.-Fiz. Zh.*, **75**, No. 1, 54–60 (2002).
10. S. A. Isaev, P. A. Baranov, N. A. Kudryavtsev, et al., Simulation of a circulation laminar flow around a square cavity with a mobile boundary at high Reynolds numbers with the use of the VP2/3 and FLUENT packages, *Inzh.-Fiz. Zh.*, **78**, No. 4, 163–179 (2005).
11. P. J. Roache, *Computational Fluid Dynamics* [Russian translation], Mir, Moscow (1982).
12. A. M. Gosmen, V. M. Pan, A. K. Ranchel, et al., *Numerical Methods for Studying Viscous Fluid Flows* [in Russian], Mir, Moscow (1972).
13. V. M. Paskonov, V. I. Polezhaev, and L. A. Chudov, *Numerical Simulation of Heat and Mass Transfer Processes* [in Russian], Nauka, Moscow (1984).
14. I. A. Belov, I. P. Ginzburg, and S. A. Isaev, Motion and heat transfer in a closed region in the presence of mobile boundaries, *Vestn. Leningr. Gos. Univ.*, No. 13, 41–50 (1976).
15. M. A. Leschziner, Practical evaluation of three finite difference schemes for the computation of steady-state recirculating flows, *Comput. Methods Appl. Mech. Eng.*, **23**, No. 3, 293–312 (1980).
16. A. Arakawa, Computational design for long-term numerical integration of the equation of fluid motion: Two-dimensional incompressible flows, Pt. 1, *J. Comput. Phys.*, **1**, No. 1, 119–143 (1966).
17. I. A. Belov and S. A. Isaev, Circulation motion of liquid in a rectangular cavity at average and high Reynolds numbers, *Zh. Prikl. Tekh. Fiz.*, No. 1, 41–45 (1981).
18. R. K. Agarwal, A third-order-accurate upwind scheme at high Reynolds number, *AIAA Paper*, Nos. 81–0112 (1981).
19. B. P. Leonard, A stable and accurate convective modeling procedure based on quadratic upstream interpolation, *Comput. Methods Appl. Mech. Eng.*, **19**, No. 1, 59–98 (1979).
20. E. Erturk, T. C. Corke, and C. Gökcöl, Numerical solutions of 2-D steady incompressible driven cavity flow at high Reynolds numbers, *Int. J. Numer. Methods Fluids*, **48**, 747–774 (2005).
21. S. Patankar, *Numerical Methods for Solving Problems of Heat Transfer and Fluid Dynamics* [in Russian], Énergoatomizdat, Moscow (1984).
22. I. A. Belov, S. A. Isaev, and V. A. Korobkov, *Problems and Methods of Calculating Separation Incompressible Fluid Flows* [in Russian], Sudostroenie, Leningrad (1989).
23. J. H. Ferziger and M. Peric, *Computational Methods for Fluid Dynamics*, Springer–Verlag, Berlin–New York (2002).
24. S. A. Isaev and A. E. Usachov, Numerical simulation of separation flows in the problems of internal aerodynamics, in: *Industrial Aerodynamics, Mechanical Engineering*, Issue 4 (36), 43–75 (1991).
25. H. B. Squire, Note on the motion inside a region of recirculation (cavity flow), *J. R. Aeronaut. Soc.*, **60**, No. 543 (1956).
26. O. R. Burggraf, Analytical and numerical studies of structure of steady separated flows, *J. Fluid Mech.*, **24**, Pt. 2, 113–151 (1966).
27. S. M. Rhi and U. L. Chou, Numerical calculation of a turbulent flow around a profile with separation at the trailing edge, *Aérokosm. Tekh.*, **2**, No. 7, 33–43 (1984).
28. S. A. Isaev, N. A. Kudryavtsev, and A. G. Sudakov, Numerical modeling of a turbulent incompressible viscous flow along bodies of a curvilinear shape in the presence of a mobile shield, *Inzh.-Fiz. Zh.*, **71**, No. 4, 618–631 (1998).
29. H. Jasak, *Error Analysis and Estimation for the Finite Volume Method with Applications to Fluid Flows*, PhD Thesis, Imperial College, University of London (1996).
30. A. A. Gavrilov, A. V. Minakov, A. A. Dekterev, and V. Ya. Rudyak, Numerical algorithm for simulation of steady-state laminar flows of Newtonian fluids in a circular gap with an eccentricity, *Vychisl. Tekhnol.*, **17**, No. 1, 44–56 (2012).
31. <http://sigma-cfd.ru/gavand/>

32. S. A. Isaev and A. I. Leont'ev, Numerical simulation of the vortex intensification of the heat transfer in a turbulent flow around a spherical dimple on the wall of a narrow channel, *Izv. Ross. Akad. Nauk, Teplofiz. Vys. Temp.*, **41**, No. 5, 755–770 (2003).
33. A. A. Gavrilov, *Computational Algorithms and a Complex of Programs for Numerical Simulation of Flows of Generalized Newtonian Fluids in a Circular Channel*, Candidate's Dissertation (in Mathematics), Inst. Teplofiziki im. S. S. Kutateladze SO RAN, Novosibirsk (2013).
34. N. Beckmann, H. P. Kriegel, R. Schneider, and B. Seeger, The R*-tree: an efficient and robust access method for points and rectangles, *Proc. ACM-SIGMOD Int. Conf. Management Data*, Atlantic City, NJ (1990), pp. 322–331.
35. A. Pascau and N. Garcia, Consistency of SIMPLEC scheme in collocated grids, *V European Conf. Comput. Fluid Dynamics "ECCOMAS CFD 2010,"* Lisbon, Portugal (2010).
36. R. S. Schreiber and H. B. Keller, Driven cavity flow by efficient numerical techniques, *J. Comput. Phys.*, **49**, No. 3, 310–333 (1983).